Contract No:

This document was prepared in conjunction with work accomplished under Contract No. DE-AC09-08SR22470 with the U.S. Department of Energy (DOE) Office of Environmental Management (EM).

Disclaimer:

This work was prepared under an agreement with and funded by the U.S. Government. Neither the U. S. Government or its employees, nor any of its contractors, subcontractors or their employees, makes any express or implied:

1) warranty or assumes any legal liability for the accuracy, completeness, or for the use or results of such use of any information, product, or process disclosed; or
2) representation that such use or results of such use would not infringe privately owned rights; or
3) endorsement or recommendation of any specifically identified commercial product, process, or service.

Any views and opinions of authors expressed in this work do not necessarily state or reflect those of the United States Government, or its contractors, or subcontractors.

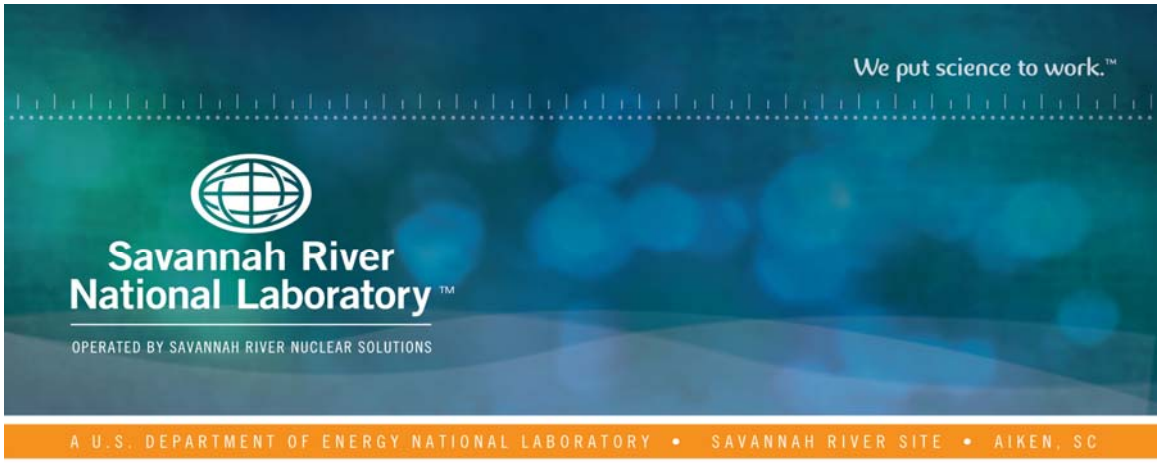

Thermal Evaluations for Mixed Organic and Nitrate Salt Drums in Interim Storage at the WCS Federal Waste Facility

Si Young Lee

February 2018

SRNL-STI-2018-00095 Revision 0

DISCLAIMER

This work was prepared under an agreement with and funded by the U.S. Government. Neither the U.S. Government or its employees, nor any of its contractors, subcontractors or their employees, makes any express or implied:

1. warranty or assumes any legal liability for the accuracy, completeness, or for the use or results of such use of any information, product, or process disclosed; or
2. representation that such use or results of such use would not infringe privately owned rights; or
3. endorsement or recommendation of any specifically identified commercial product, process, or service.

Any views and opinions of authors expressed in this work do not necessarily state or reflect those of the United States Government, or its contractors, or subcontractors.

Printed in the United States of America

Prepared for
U.S. Department of Energy

SRNL-STI-2018-00095
Revision 0

Keywords: *Thermal Evaluations, CFD Modeling Approach, Standard Waste Box*

Retention: *Permanent*

Thermal Evaluations for Mixed Organic and Nitrate Salt Drums in Interim Storage at the WCS Federal Waste Facility

Si Young Lee

February 2018

Prepared for the U.S. Department of Energy under contract number DE-AC09-08SR22470.

Savannah River National Laboratory™
OPERATED BY SAVANNAH RIVER NUCLEAR SOLUTIONS

REVIEWS AND APPROVALS

AUTHORS:

S. Y. Lee, Environmental Modeling Date

TECHNICAL REVIEW:

M. R. Kesterson, Tritium Process Science Date

APPROVAL:

D. A. Crowley, Manager Date
Environmental Modeling

L. T. Reid, Director Date
Environmental Restoration Technology

S. D. Fink, Advisory Manager Date
Chemical Processing Technologies

EXECUTIVE SUMMARY

Waste Control Specialists LLC (WCS) operates the Federal Waste Facility (FWF) in Texas that is licensed to process and store certain types of mixed low-level radioactive waste packages. The specific waste currently housed at WCS includes some of the transuranic (TRU) waste that originated at the DOE Los Alamos National Laboratory (LANL) and are destined for disposal at the DOE Waste Isolation Pilot Plant (WIPP) facility. The TRU waste within each Standard Waste Box (SWB) was packaged in 55-gallon drums at LANL. Some of the drums contain mixed organic and nitrate salt contents suspected of experiencing a chemical reaction. The drums (up to four drums in a SWB) were then overpacked in a SWB prior to shipment to WCS. In the most common configuration, WCS placed the SWB containing the drums on metal pallets and stored two SWBs into Modular Concrete Canisters (MCCs) in a double stacked array. The MCCs were placed in a staggered array at a segregated area of the FWF and covered with sand to mitigate the heating that occurred when stored above ground on waste pads. The temporary interment is also intended to provide additional containment of the suspect reactive waste to mitigate release of radioactivity in an incident such as that which occurred at WIPP for one such drum. Void space of each MCC was filled with 1-inch pea gravel to facilitate retrievability. Thermocouple probes were placed within each MCC to monitor heat generation from the SWBs and the MCC lids were closed. The primary objective of this analysis was to estimate the heat generation of the SWB drum contents when the SWB package temperature inside the MCC and the FWF ambient temperature were monitored.

A three-dimensional steady-state computational approach was taken to achieve the objective. The computational model was benchmarked for a simplified geometry representing the waste heat dissipation for a retrievable underground waste package. The benchmarking results demonstrated that the modeling results for temperature distribution are in excellent agreement with the theoretical results to within about 0.1%.

The symmetrical boundary conditions for the modeling domain were used for computational efficiency. The impact of the symmetry assumption was assessed in terms of thermal evaluations by changing the asymmetrical geometry to the symmetrical one. The assessment results showed that the thermal impact due to the symmetrical boundary of the prototypic SWB geometry was found to be negligible.

The thermal calculations for the four different test periods as monitored by WCS were made to estimate the heat source generated by the chemical reactions of the SWB contents when the SWB wall temperature and ambient temperature of FWF for each of the test cases were provided. The calculation results showed that the reaction heats for the WCS drum contents ranged from about 3 watts to 20 watts when the surface temperatures of the SWB stored inside the MCC container were monitored in the range of 88^{o} F to 138^{o} F under the solar condition. In addition, the sensitivity results showed that when solar heat was included at the ground surface of the WCS facility, the calculated temperature at the probe point reached the measured value for each of the test cases at the SWB heat source about 16 watts lower than that of the case without the solar heat. The sensitivity results for the soil temperatures of the domain boundary indicated that when the soil temperature was 5^{o}F lower than the nominal value of 68^{o}F, total heat of the SWB was estimated to be about 1 watt higher than the nominal one under the solar condition. Changing the thermal conductivity of the waste from the assumed value of 0.65 W/m-K to the sensitivity value of 0.45 W/m-K results in a reduction of the reaction drum heat of less than 0.5 watt for the test cases documented in this report.

TABLE OF CONTENTS

LIST OF TABLES

LIST OF FIGURES

LIST OF ABBREVIATIONS AND NOMENCLATURE

CFD	Computational Fluid Dynamics
FWF	Federal Waste Facility
LANL	Los Alamos National Laboratory
MCC	Modular Concrete Canister
SWB	Standard Waste Box
TRU	Transuranic
WCS	Waste Control Specialists LLC
A_w	Wall surface area
C_p	Specific heat
d	Wall thickness
°F	degrees Fahrenheit
ft	British length unit (1 ft = 0.3048m)
h	Heat transfer coefficient
in	inch (1 inch = 0.0254m)
k	Thermal conductivity
$k_{b,eff}$	Thermal conductivity for waste contents
k_w	Thermal conductivity for wall
L	Length scale
m	SI length unit (meter)
q_{cond}	Conductive heat flux
q_{rad}	Radiative heat flux
q'''	Heat source per unit volume
r	Local radius of circular cylinder
R	Radius of circular cylinder
T	Absolute temperature
T_{amb}	Ambient temperature
T_m	Maximum temperature
T_s	Surface temperature for inner wall
T_w	Wall surface temperature
u_i	Velocity along the i-direction (u for i = 1, v for i =2, and w for i =3 in case of Cartesian coordinate system)
V_b	Volume of wall
x_i	Coordinate system (x for i = 1, y for i =2, and z for i =3 in case of Cartesian coordinate system)
X	Gravity term in momentum balance equation
$\bar{v}$	Natural convection velocity
∇	Gradient operator
σ	Shear stress tensor or Stefan-Boltzmann constant (=5.670373 x 10^{-8} W/m^2K^4)
ε	Surface emissivity
θ	Ratio of local temperature to maximum temperature with respect to wall temperature
η	Non-dimensional and local radial distance (=(r/(R+d))
η_R	Non-dimensional radial distance (=(R/(R+d))
ρ	Density
λ_k	Ratio of thermal conductivities

1.0 Introduction

Waste Control Specialists LLC (WCS) operates a facility in Texas that is licensed to process and store certain types of mixed radioactive waste packages. The currently stored waste includes some of the transuranic (TRU) waste that originated at the DOE Los Alamos National Laboratory (LANL) and are destined for disposal at the DOE Waste Isolation Pilot Plant (WIPP) facility. Prior to the 2014 WIPP incident of a fire with this type of waste, WCS began receiving LANL TRU waste and intended to temporarily store the LANL waste at the WCS facility. The TRU waste within each Standard Waste Box (SWB) was packaged in Type A 55-gallon drums at LANL prior to shipment to WCS. WCS placed some of the SWBs containing the drums of the identified LANL waste on metal pallets and stored two SWBs into Modular Concrete Canisters (MCCs) in a double stacked array as shown in Fig. 1. WCS also packed the material into larger MCCs containing up to four SWBs. The current analysis focused on the MCC configuration containing two SWBs.

Figure 2 shows two SWBs separated by 4-inch metal pallet inside the cylindrical MCC container. The void space of each MCC was filled with washed pea gravel to ensure retrievability. Thermocouples were placed within each MCC to monitor heat generation from the SWBs and the MCC lids were closed. The temperature in each MCC is monitored to provide an indication for reactivity change of the WCS drums. As shown in Fig. 2, one of the thermocouple probes for the temperature measurements of each SWB is located on the side surface of the metal pallet between two stacked SWBs. All the thermocouples were connected to a central location for daily monitoring. The MCCs were carefully moved and placed in a staggered array at a segregated area of the FWF and covered with sand to act like a filter should an exothermic event occur that compromises the drum and potentially allows release of radioactive isotopes [1]. The staggered arrangements of the MCCs are shown in Fig. 3. WCS then poured a one-foot, flowable sand layer around and over the MCCs as shown in Fig. 2.

The primary objective of this work was to evaluate thermal performance for 55-gallon drums stored in an enclosed SWB, located inside the underground MCC. The evaluation uses a computational approach for a modeling domain as defined in an approximately representative manner. For this work, symmetrical domain and lumped-source term approaches were used for a computational efficiency.

Table 1 provides additional information on the modeling inputs and assumptions. Table 2 contains the assumed material and physical properties.

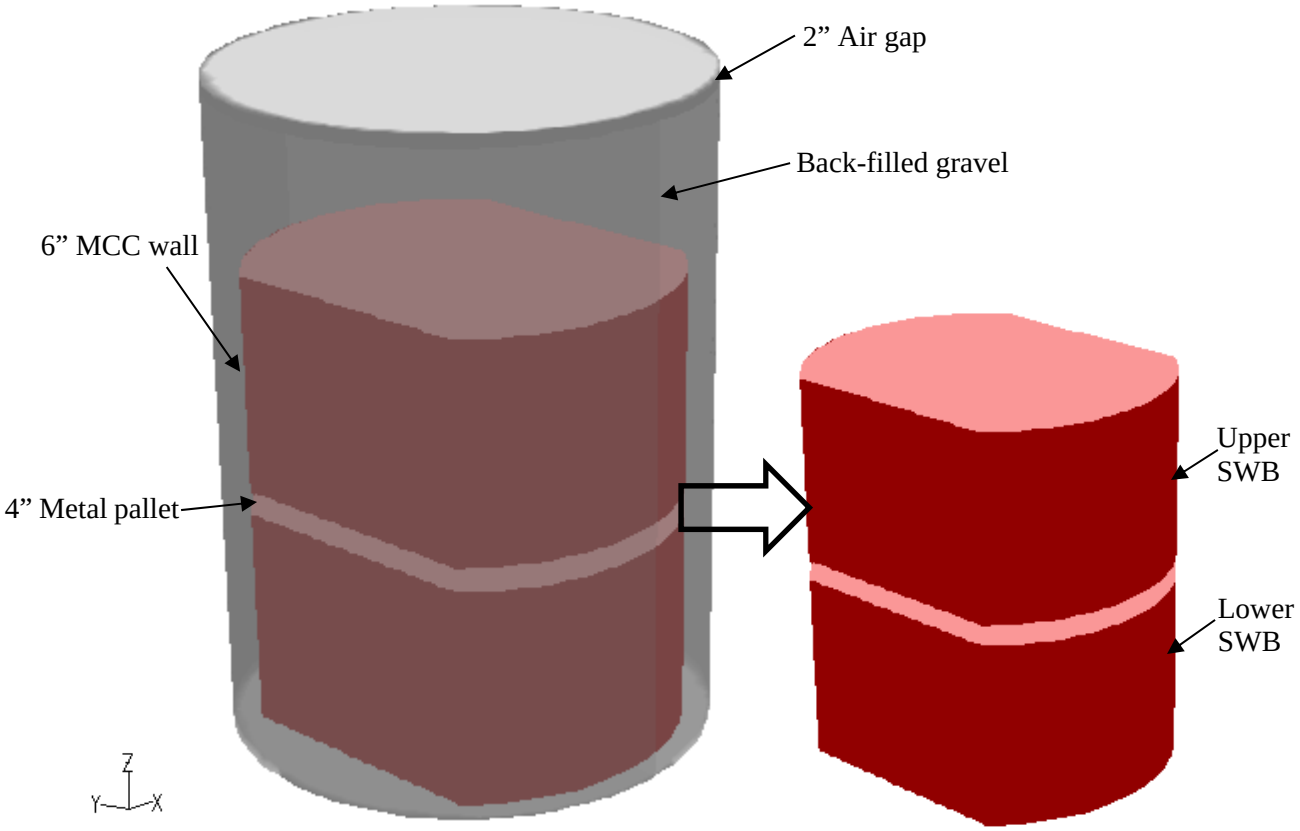

Figure 1. Two SWBs containing heat generation sources inside a cylindrical MCC

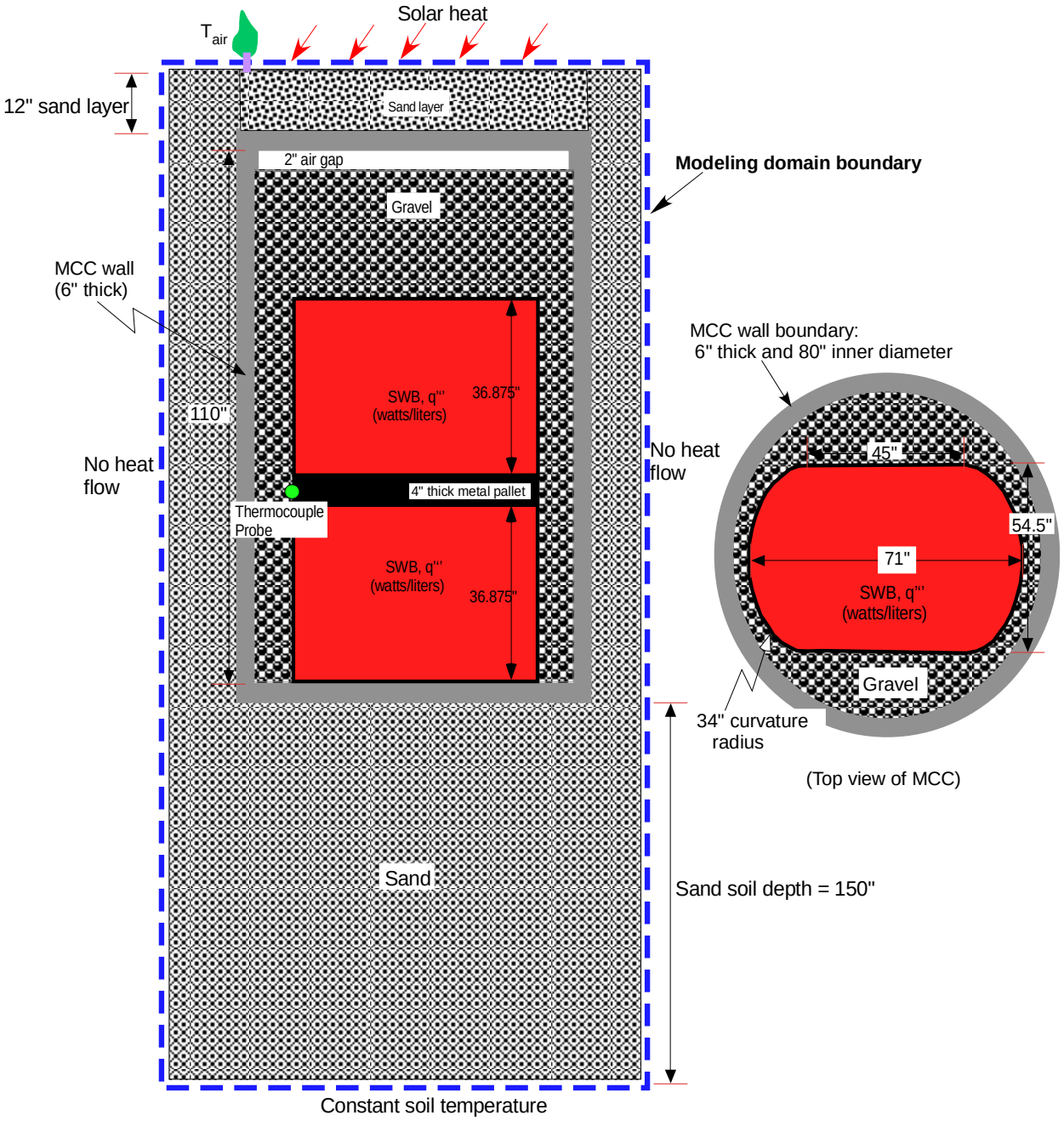

(Side view of modeling domain)

Solar heat: 340 watts/m^2 incoming solar heat, but 48% of the solar heat absorbed at the ground surface, (Ref.:Data from NASA Earth Observatory)

Figure 2. Modeling domain and geometry including 4-inch metal pallet [3]

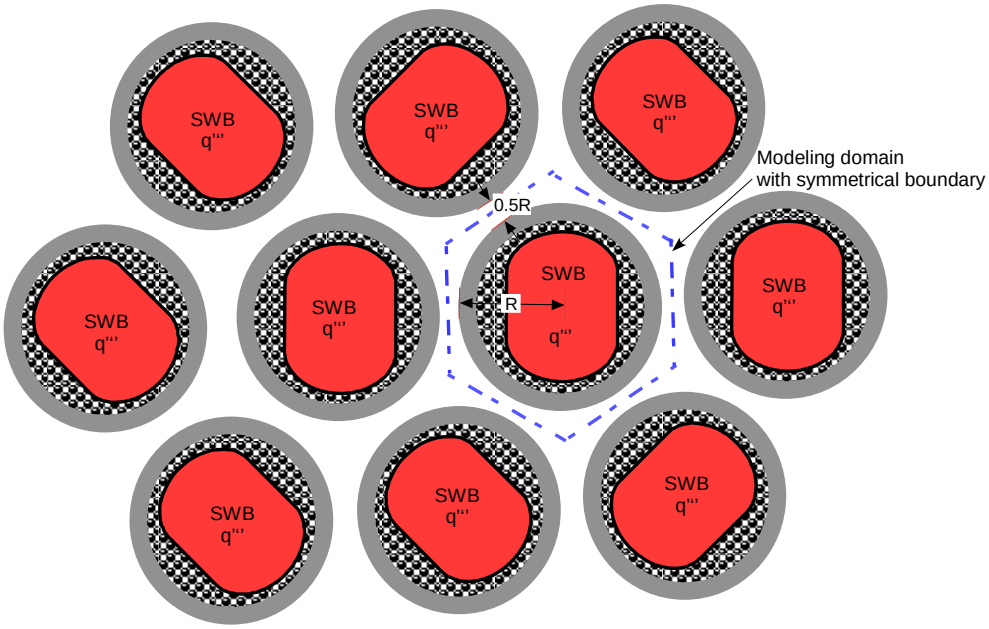

Figure 3. Top view of a staggered array of MCC containers

Table 1. Modeling conditions used for the calculations

Input Parameters	Modeling Data	
Standard Waste Box (SWB) geometry and dimensions (See Fig. 1 and Fig. 2) [3]	Rectangular container with round edges (Carbon steel)	Inside: 36.56 in high, 68.75 in long, 52 in wide Outside: 36.875 in high, 71 in long, 54.5 in wide
SWB contents	Salt solution	
Modular Concrete Canister (MCC) [3]	Cylindrical geometry (Concrete)	Internal diameter: 80 in Wall thickness: 6 in
MCC back-fill materials	Gravel	
Burial depth of MCC [3]	12 in as shown in Fig. 2	
Back-fill material to the ground level around MCC	Dry sand	
Soil thermal penetration depth	Annually averaged: ~150 in [2]	
MCCs placement layout	Staggered array (See Fig. 3)	
Ambient temperature during storage	Measurement data provided by WCS	
Solar heat above the FWF ground surface	340 watts/m^2 heat flux for top ground surface (from NASA Featured Article), and 48% absorbed at the ground surface [5]	

Table 2. Material and thermal properties used for the nominal steady-state calculations

Material	Thermal conductivity (W/m-K)	Surface emissivity
Air layer [10]	0.0242	-
MCC (Concrete) [12]	1.4	-
Carbon steel (SWB drum) [11]	43	0.3
SWB contents* [4]	0.65	-
Dry sand [9,11]	0.25	0.76
Gravel (dry) [13]	0.4	-

Note:*0.45 W/m-K used for sensitivity calculation

2.0 Modeling Geometry and Approach

The computational heat transfer approach uses a commercial finite volume Computational Fluid Dynamics (CFD) code, ANSYS-FLUENT™ [6], as a tool to create a prototypic geometry file under a non-orthogonal mesh environment in the body-fitted coordinate system. The geometrical dimensions of the WCS storage components and the modeling domain are shown in Fig. 2. A three-dimensional modeling geometry was created and meshed using the ANSYS preprocessor software. The computational volume of the modeling domain is decomposed into component surfaces that allow greater mesh accuracy and efficiency. In regions expected to experience larger temperature gradients and/or increased material density gradients, the component surface is assigned a greater mesh density to increase thermal solution accuracy. The gas-filled regions of the container are examples of component surfaces with greater mesh density, as well as regions on and near conducting/convecting/radiating surface boundaries. Conversely, the mesh density is reduced on component surfaces expected to experience smaller temperature gradients; such as the gravel portions of the MCC package and thick soil layer surrounding the waste container. This approach to modeling and meshing the MCC package decreases the computational time and increases the solution accuracy. As shown in Fig. 3, the symmetrical and adiabatic boundary conditions for the modeling domain were used for computational efficiency. The symmetry involved is approximately the SWB with an equivalent cylinder volume. In this case, an asymmetrical impact of the SWB geometry was assessed in terms of thermal evaluations by converting the asymmetrical geometry to the symmetrical one as shown in Fig. 4. During the symmetrical process, the package volume of the SWB was kept unchanged.

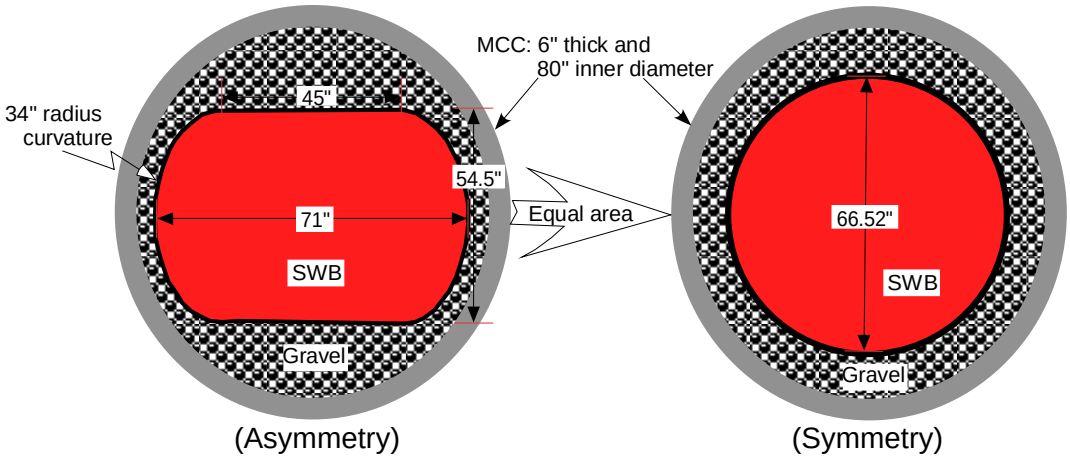

Figure 4. Symmetry process of asymmetrical SWB geometry inside MCC

The steady-state three-dimensional equation governing the heat transfer problem of the SWB in the MCC under the Cartesian coordinate system is shown below.

When thermal evaluations are made for the MCC packages buried at the FWF, the steady-state energy balance equation under the Cartesian coordinate system is applied as shown below [3].

$$\rho C_p u_j \frac{\partial T}{\partial x_j} - \sum_{i=1}^{3} \left\{ \frac{\partial}{\partial x_i} \left(k \frac{\partial T}{\partial x_i} - q_{r,i} \right) \right\} - q''' = 0 \qquad (1)$$

Natural convection term for the first term in Eq. (1) is neglected for a conservative estimate because local air velocity u_j induced by the air temperature gradient inside the enclosed MCC container is assumed small. Scoping results show that the temperature change due to the radiation heat flux term $q_{r,i}$ in the equation was found to be smaller than 0.2°C under the current range of low-level energy sources.

The heat source term *q'''* is provided to the energy equation as a model input. Complete setup of the modeling calculations requires the input parameters such as thermal and material properties of the storage components, heat source term, boundary conditions, and domain discretization, along with the established modeling domain and assumptions. These are discussed subsequently.

2.1 Solution Approach and Assumptions

A three-dimensional steady-state CFD approach was taken for thermal evaluations of the underground SWB package in the interim FWF storage facility. A prototypic package geometry for the facility was modeled for the thermal calculations as shown in Fig. 2. As shown in the figure, the facility consists of an array of cylindrical MCCs. Each MCC contains two SWBs placed on a pallet in a double stacked array as shown in Fig. 1. Thus, the cylindrical MCC has the upper and lower SWBs. Each SWB contains four drums of waste contents at maximum loading. The heat source in each drum is the sum of two contributions. They are radiolytic decay heat and reaction heat. The radiolytic heat is essentially constant and independent of local temperature, while the reaction heat is dependent on temperature and is directly related to the chemical reactions of salt waste

contents. From the measurement records [8], the radiolytic heat sources are 1.689 watts for the upper SWB and 1.163 watts for the lower SWB. The upper SWB contains only the radiolytic heat without any mixed organic and nitrate salt drums suspected of chemical reaction. Hence, the lower SWB has only two drums suspected as susceptible to producing chemical reaction heat. For simplicity, this analysis assumes the drums are reacting identically.

The primary objective of the work is to estimate the heat source resulting from the chemical reactions of the drum contents contained in the SWB when the temperature of the SWB wall surface along with ambient temperature is obtained by the thermocouple probe as shown in Fig. 2.

Main approach and assumptions used for the present work are made as follows.

- All modeling calculations were based on quasi steady state conditions for each respective time period calculated.
- Prototypic geometry for the WCS SWB storage facility was created and discretized by using the boundary-fitted coordinate system under a three-dimensional CFD domain.
- The lower SWB has two 55-gallon drums containing identical reactive heat sources, but the upper SWB has no reactive heat source.
- Heat source of waste contents is uniformly distributed over the entire domain of each SWB.
- Solar heat was considered by using NASA data: 340 watts/m^2 and 48% of the heat absorbed at the ground surface based on 12-hour period [5].
- Soil region below the SWB storage facility was included with 150-inch soil depth, and the bottom boundary of the soil region could be kept constant, 68^{o}F [2]. In this case, another temperature of 63^{o}F was applied to the soil boundary for the sensitivity assessment of the calculated thermal source term for the waste contents.
- Material and thermal properties are assumed to be constant because this work is applied to the low temperature gradient of TRU waste package.
- Heat flow to the adjacent MCC domain boundary was neglected for ease of calculations, assuming MCCs to be placed in an infinite staggered array as shown in Figs. 2 and 3. Thus, top region of the computational domain is cooled by natural convection and radiation under ambient temperature [15], and the bottom region of the domain is cooled down to an infinite heat sink of soil region.

Based on the solution approach and assumptions, a computational domain was defined as shown in Fig. 2. A steady-state CFD solution method was applied to a discretized domain of the prototypic MCC geometry in the body-fitted coordinate system to achieve the objective. The resulting number of computational mesh nodes over the modeling domain is approximately 260,000 nodes. Figure 5 illustrates the computational mesh over the three-dimensional modeling domain containing two SWB geometries. As shown in the figure, hexahedral computational meshes for the domain were used for the present calculations.

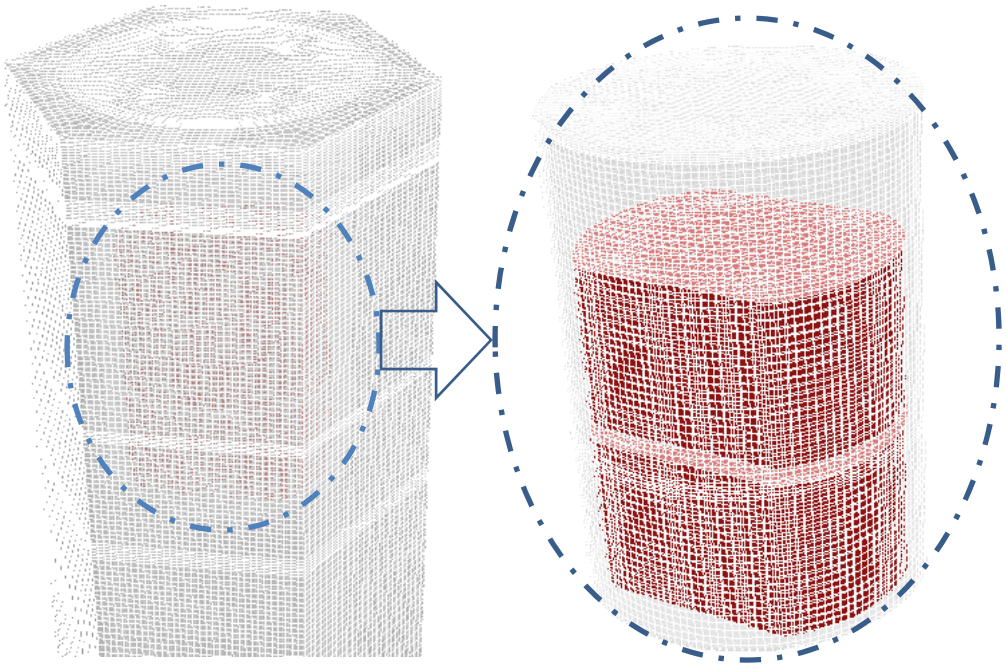

Figure 5. Computational meshes for a three-dimensional modeling domain

2.2 Modeling Cases and Boundary Conditions

For the modeling calculations, four different time periods were considered for the assessment of the waste heat sources from measurement cases during the interim SWB storage conditions as listed in Table 3. All of the cases are assumed to have all SWBs uniformly loaded with the same waste contents and to maintain the FWF facility in dry condition representative of the material and physical properties from Table 2. The lower SWB is assumed to contain the heat source equivalent to two reactive drums. As shown in Table 3, surface temperatures of a given SWB ranged from 88^{o} F to 138^{o} F, depending on the monitoring period of the interior of the MCCs and ambient temperatures of FWF.

Figure 5 shows total number of discretized meshes for the modeling domain, which was established as 2.6x10^{5} mesh nodes for the present calculations. The boundary conditions for the discretized computational domain of Fig. 2 are listed in Table 4. Typical computational time for the current modeling domain required about a couple of hours when four cpu's were used in a parallel way under SRNL high performance computing platform.

For the calculations, a commercial CFD software, ANSYS-FLUENT [6], was applied to the modeling domain. The benchmarking test related to the current thermal model was made as a typical case representing a physically dominant cooling mechanism. It is also noted that the software is separately benchmarked to meet the SRS software quality requirements (referring to 1Q Manual, QAP 20-1) that consist of level-B Software Quality Assurance Plan and a Test Plan that includes a number of problems and solutions from text books, references, and the literature test results [7].

Table 3. Modeling conditions for the measurement periods of MCC C-0271

Measurement cases	Measured values (Effective mean temperature)	
	Mean ambient air temperature (°F)	Temperature at the probe point between two SWBs (°F)
2Q-2014	74.0	138.1
3Q-2015	81.5	111.1
4Q-2016	56.5	88.1
2Q-2017	72.0	106.5

Table 4. Quasi-steady state boundary conditions for the calculations

Components	Modeling conditions
Domain side boundary	No heat flow at the side boundary of the modeling domain as shown in Fig. 3 and Fig. 4
Thermal penetration depth into the dry sandy soil	Annually ~150" depth (used for the present analysis) [2]
Domain bottom boundary	Constant soil temperature (68°F) at the bottom boundary of the modeling domain (150" beneath the bottom of MCC [2]) as shown in Fig. 4
Top surface boundary conditions	Ambient air temperature from data, 340 watts/m^2 heat flux for top ground surface (from NASA data), and 48% absorbed at the ground surface based on 12-hour period [5]
Measurement probe location	Measurement data at the side mid-point of two SWB's pallet layer (4" thick metal pallet) (See Fig. 2)

3.0 Benchmarking Test for the Thermal Model

A theoretical approach for steady-state conduction heat transfer of a multi-layered cylinder containing a heat generation source q''' was taken to verify the present thermal model for a simplified waste container with heat generation as shown in Fig. 6. These evaluations were made to benchmark and verify the current model. The theoretical model was based on one-dimensional approach. Under steady-state conditions, the energy balance of Eq. (1) for the waste contents region with effective thermal conductivity $k_{b,eff}$ becomes

$$k_{b,eff}\nabla^2 T + q''' = 0 \qquad (2)$$

For the waste region with a uniformly distributed heat generation source q''' as shown in Fig. 8, Eq. (2) becomes

$$\frac{d^2T}{dr^2} + \frac{1}{r}\frac{dT}{dr} + \frac{q'''}{k_{b,eff}} = 0 \tag{3}$$

As boundary conditions, the following relations at the center and wall of the waste contents region are applied to the above equation, Eq. (3).

$$\left.\frac{dT}{dr}\right|_{r=0} = 0 \tag{4}$$

$$T(r = R) = T_s \tag{5}$$

After integrating Eq. (3) and applying the boundary conditions, the radial temperature distribution for the waste container with heat generation source q''' becomes

$$T(r) = T_s + \frac{q'''}{4k_{b,eff}}\left(R^2 - r^2\right) \quad (0 \le r \le R) \tag{6}$$

Equations governing the steel wall region $(R \le r \le (R + d))$ with no heat source (q'''=0) are

$$\frac{d^2T}{dr^2} + \frac{1}{r}\frac{dT}{dr} = 0 \tag{7}$$

Boundary conditions at the wall of the waste canister are

$$T\left(r = (R + d)\right) = T_w \tag{8}$$

and

$$q''_w = -k_w \left.\frac{dT}{dr}\right|_{r=(R+d)} = h_w\left(T_w - T_\infty\right). \tag{9}$$

where d is the steel wall thickness of the waste container, and k_w is thermal conductivity of steel wall.

In Eq. (9) the wall heat flux (q''_w) can be obtained by the energy balance between the heat source and the heat sink when the volumetric heat source q''' is spatially uniform in Region-I of Fig. 8. The resulting equation for the wall heat flux is

$$q''_w = q'''\left(\frac{V_b}{A_w}\right) = q'''\left\{\frac{\pi R^2 L}{2\pi(R + d)L}\right\} = q'''\left\{\frac{R^2}{2(R + d)}\right\} \tag{10}$$

where A_w is the area of the wall and V_b is the volume of wall. Using Eqs. (8), (9), and (10), the radial temperature distribution of the container wall region with no heat source (q'''=0) becomes

$$T(r) = T_w + \frac{q''_w (R+d)}{k_w} ln\left(\frac{R+d}{r}\right)$$
$$= T_w + \frac{q''' R^2}{2k_w} ln\left(\frac{R+d}{r}\right) \qquad (R \le r \le (R+d)) \tag{11}$$

The inner surface temperature of the container can be evaluated by Eq. (11). That is,

$$T_s = T_w + \frac{q''' R^2}{2k_w} ln\left(\frac{R+d}{R}\right) \tag{12}$$

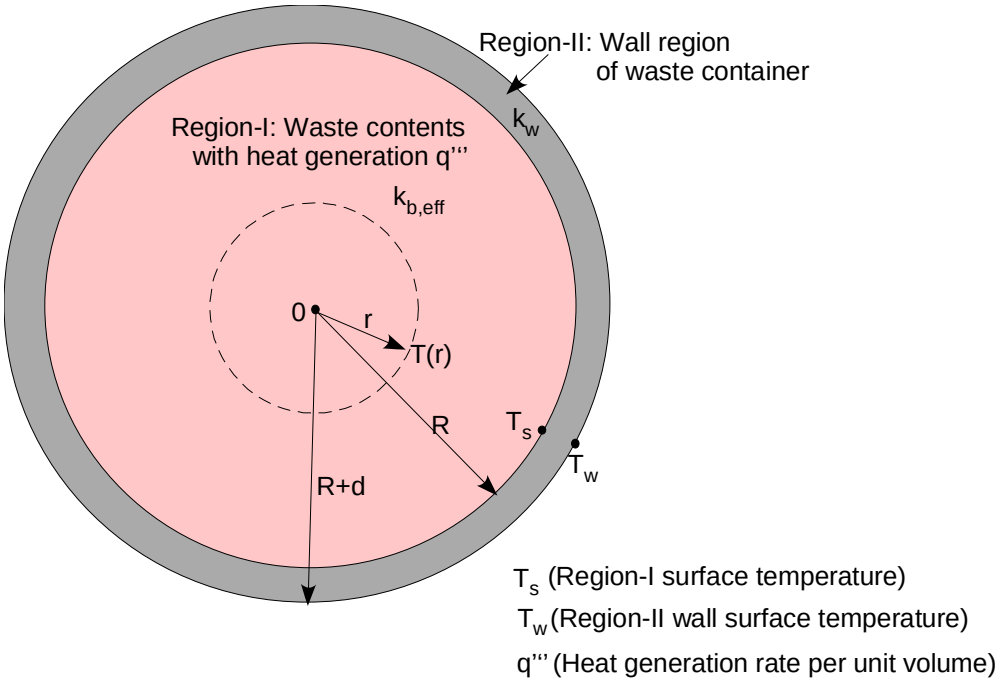

Figure 6. Graphical illustration of the thermal model of the simplified waste container containing a heat generation source q'''.

From Eqs. (6) and (12), the temperature of the waste region can be obtained in terms of the ambient temperature.

$$T(r) = T_w + \left(\frac{q''' R^2}{2k_w}\right) \ln\left(\frac{R+d}{R}\right) + \frac{q'''}{4k_{b,eff}} \left(R^2 - r^2\right) \tag{13}$$

At r = 0, maximum temperature difference ($T_m - T_w$) becomes

$$(T_m - T_w) = \left(\frac{q''' R^2}{2k_w}\right) \ln\left(\frac{R+d}{R}\right) + \frac{q''' R^2}{4k_{b,eff}} \tag{14}$$

When wall surface temperature is measured, the temperature distribution for the waste region as shown in Fig. 6 can be non-dimensionalized in terms of the container wall temperature difference (T_m -T_w) and the container radius (R+d) to examine the impacts of the design parameters on the temperature distributions of the waste contents. Non-dimensional parameters for radial distance and temperature are defined as follows:

$$\eta(r)=\frac{r}{(R+d)} \text{ and } \theta=\frac{(T-T_w)}{(T_m-T_w)} \quad (15)$$

Temperature and length scales are non-dimensionalized in terms of the temperature difference (T_m -T_w) and the container radius (R+d) as shown in Eq. (15).

For a waste region ($0 \le \eta \le \eta_R \left(=\frac{R}{(R+d)}\right)$), the non-dimensional temperature distribution for the waste contents region can be obtained from Eqs. (14) and (15).

$$\theta(\eta)=1-\left(\frac{0.5\lambda_k}{0.5\lambda_k-\ln(\eta_R)}\right)\left(\frac{\eta}{\eta_R}\right)^2 \quad (16)$$

Non-dimensional number λ_k in Eq. (16) is defined as the thermal conductivity ratio of the container wall to waste contents region. That is

$$\lambda_k=\frac{k_w}{k_{b,eff}} \quad (17)$$

Thus, a very low value for the λ_k number means that internal conduction resistance is negligible in comparison with container wall resistance. This in turn implies that the waste temperature will be nearly uniform throughout the container.

Thus, the non-dimensional temperature distributions for the waste contents can be computed, and they can be compared with the steady-state calculation results to verify the modeling predictions. In this case, the solution was obtained by solving the steady-state energy balance equation in Eq. (2). Eq. (16) shows that the maximum temperature gradient is closely related to the ratio of thermal conductivity for the container wall region to the effective thermal conductivity of the waste contents as expected. For a given geometry and wall cooling conditions, the effective thermal conductivity is found to be the key parameter to control the maximum temperature difference between the waste contents center and its wall.

When the thermal properties of the waste contents and concrete wall remain constant and the volumetric heat load is 0.01 watts/liter for the purpose of benchmarking, the steady-state temperature differences for the waste contents between the container center and wall are compared for a given size of the waste container, 80 inches in diameter. The heat load applied here is in the range of the SWB waste contents. Figure 7 shows comparisons of theoretical values with the present modeling results for the verification of the present thermal model. As compared in the figure, it is demonstrated that the calculated results for the maximum temperature are in excellent agreement with the theoretical results to within about 0.1%.

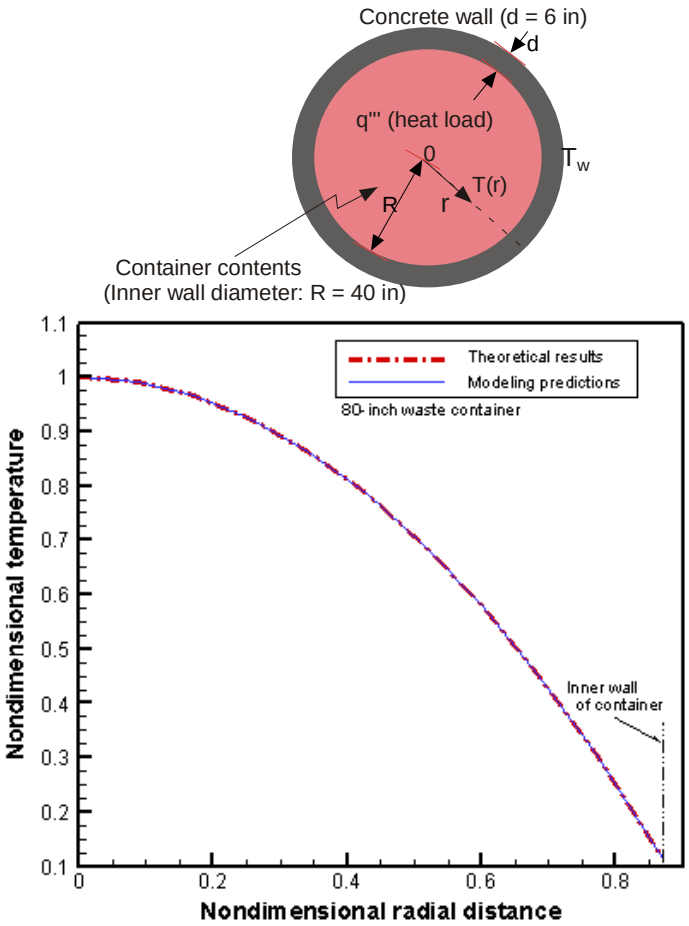

Figure 7. Comparison of steady state results between the modeling and theoretical results for the cylindrical waste container with 0.01 watts/liter heat load for the model benchmarking (Note that non-dimensional parameters are defined in Eq. (15)).

4.0 Results and Discussions

The benchmarking test for the current computational model was made as a typical case representing the waste heat dissipation for a retrievable underground waste package because the test case is closely related to the underground cooling mechanism of WCS drums in an interim waste disposal facility of FWF. Based on the solution methodology and the modeling assumptions as discussed earlier, a three-dimensional steady-state CFD approach was taken to compute temperature distributions for the discretized computational domain of the MCC region containing two SWBs as shown in Fig. 2. In this work, boundary conditions provided in Table 4 were imposed on the modeling domain for the thermal calculations of the modeling cases.

For the analysis, four time periods were selected for the modeling calculations from the measurement data sets as shown in Table 3. As shown in the table, the effective mean wall surface temperatures of the SWB package were determined 88 ^{o}F to 138 ^{o}F, depending on the monitoring period of the interior of the MCCs and ambient temperatures of FWF. The measurement probe inside the MCC is shown in Fig. 2. In the calculations,

it is assumed that SWB is uniformly filled with waste contents. Each SWB stores four drums at the most. The heat source in each drum is the sum of two contributions, radiolytic decay heat and chemical reaction heat. The radiolytic heat is essentially constant and independent of temperature, while the reaction heat depends on temperature and is directly related to the chemical reactions of nitrate salts. The measurement records indicate that total radiolytic decay heat (1.689 watts) for the upper SWB is slightly higher than that of the lower SWB (1.163 watts). The upper SWB contains only the radiolytic heat without any reaction heat. Only two drums of the lower SWB contain nitrate waste salts mixed with organic, and they have the reaction heat. The objective of the work was to estimate the heat source generated by the chemical reactions of the drum waste contents contained in the lower SWB when the SWB wall surface temperature measured by the thermocouple probe and ambient temperature of FWF are provided.

A first modeling case in Table 3, 2Q-2014, corresponds to the case of 138.1 ^{o}F for the side surface of SWB and 74 ^{o}F for ambient temperature. For this case, the boundary conditions as provided by Table 4 were applied to the computational domain of Fig. 5 to calculate the corresponding SWB heat source. When solar heat was not considered during the monitoring period, the steady state results for the 2Q-2014 case showed that the lower SWB package with heat source of 57 watts reached the measured temperature 138.1 ^{o}F at the probe point. For the MCC container containing two SWB packages under the 2Q-2014 case with the solar condition, total heat generated by the lower SWB was calculated to be about 40.5 watts including the radiolytic and reaction heats. Considering the radiolytic heat of 1.163 watts, the drum reaction heat for the case 2Q-2014 can be calculated by subtracting radiolytic heat from the calculated total heat source of 19.67 watts assuming two identical reactive drums. From the results, it is noted that when the solar heat as provided in Table 4 was applied to the ground surface, the measured temperature for the first case was reached at the SWB heat source about 16.5 watts lower than that of the shaded case. Figure 8 compares the temperature profiles along the vertical line crossing the temperature monitoring point of the SWB package for different cases under the insulated condition. Table 5 summarizes the calculation results of total SWB heats for all of the four measurement cases. Results of the drum reaction heats for the four cases are presented in Table 6. Figure 9 compares the steady-state temperature distributions for the vertical center plane between the 2Q-2014 cases with and without solar heat on the ground surface when temperature probe indicates 138 ^{o} F in an ambient temperature 74 ^{o}F. Fig. 10 compares the steady-state temperature distributions for the vertical mid-plane among the four cases with solar heat at the ground surface. The results for all of the modeling cases clearly indicate that the temperatures for the upper SWB are much lower than those of the lower one because the upper one contains only the radiolytic decay heat without any chemical reaction heat.

The symmetrical boundary conditions for the modeling domain were used for computational efficiency. In this case, an asymmetrical impact of the SWB geometry was assessed in terms of thermal performance by changing the asymmetrical geometry to the symmetrical one as shown in Fig. 4. For the symmetrical process, the SWB volume was kept unchanged for the same heat source. The test case of 2Q-2014 was chosen for the impact assessment of symmetrical boundary on the thermal performance. Table 7 provides the results that the thermal impact due to the symmetrical boundary for the asymmetrical SWB geometry was found to be negligible. For the analysis, a nominal soil temperature of 68^{o}F has been applied to the modeling domain boundary. For a sensitivity anlaysis, a soil temperature 5^{o}F lower than the nominal value was used to estimate the impact of the thermal source term contained in the SWB package. As shown in Fig. 11, the results indicate that when the lower SWB contains two identical reactive drums, total heat of the SWB is predicted to be about 1 watt higher than the nominal one for the solar

condition. Table 8 also shows a quantitative comparison for the two different soil temperatures. The nominal analysis was performed, assuming bulk thermal conductivity of the WCS salt contents to be 0.65 W/m-K. Thermal conductivity of 0.4 W/m-K for the processed solid salt was previously used for WIPP technical assessment [14]. When the bulk thermal conductivity of the waste is changed from 0.65 W/m-K to 0.45 W/m-K, total raction heat of the lower SWB for all test cases is decreased by at the most 1 watt as shown in Table 9. Figure 12 shows that this change makes the reaction drum heat shifted to at most 0.5 watts. As compared in Table 10, maximum temperature of the SWB package is increased by at the most 2°F when thermal conductivity of the SWB waste contents shifts from the assumed value of 0.65 W/m-K to the sensitivity value of 0.45 W/m-K.

From all of the modeling results, it is noted that the reaction heat for the WCS drum contents ranges from 3 watts to 20 watts when the SWB surface temperatures stored inside the interim MCC storage container are in the range of 88 °F to 138 °F.

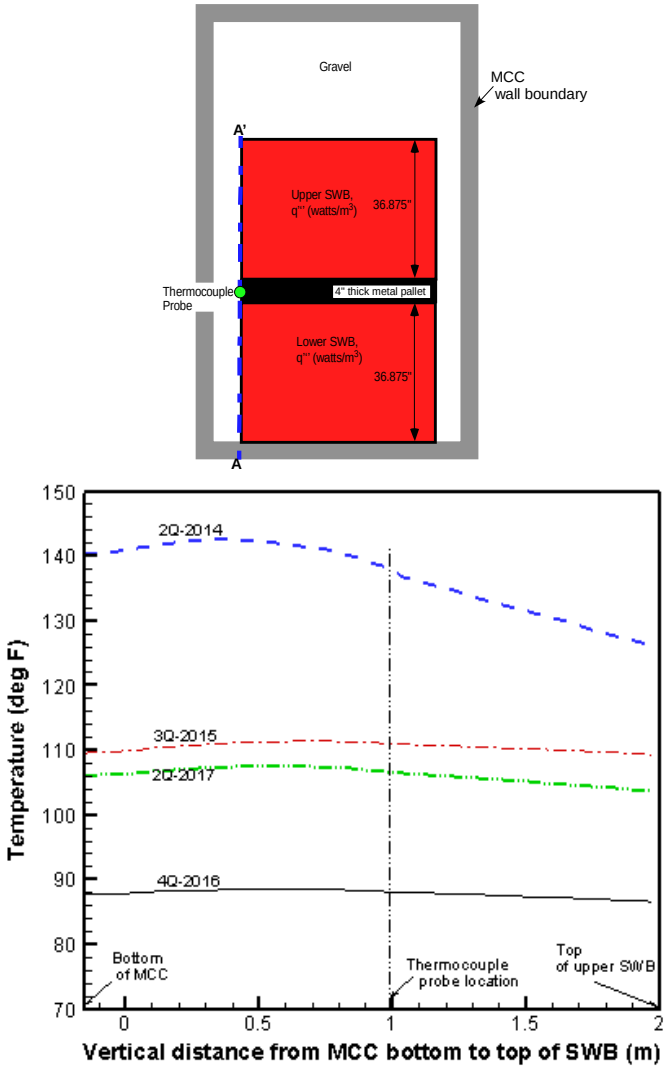

Figure 8. Temperature profiles for four different cases along the vertical line A-A' crossing the temperature measurement probe of the SWB packages with solar conditions

Table 5. Results of modeling calculations for the test conditions

Cases	Measured values (Mean temperature)		Modeling predictions			
	Ambient air temperature (°F)	Temperature at the point between two SWB's (°F)	No solar heat		Solar heat*	
			Upper SWB heat** (watts/SWB)	Lower SWB heat (watts/SWB)	Upper SWB heat** (watts/SWB)	Lower SWB heat source (watts/SWB)
2Q-2014	74.0	138.1	1.69	57.0	1.69	40.5
3Q-2015	81.5	111.1	1.69	27.5	1.69	11.7
4Q-2016	56.5	88.1	1.69	24.0	1.69	6.8
2Q-2017	72.0	106.5	1.69	30.0	1.69	13.5

Note: *Solar heat source [5]
**The upper SWB does not contain any reaction heat source.

Table 6. Results of the calculated reaction heats of Lower SWB for the test conditions[++]

Cases	Measured values (Mean temperature)		Modeling predictions (Solar heat**)		
			Lower SWB heat source		
	Ambient air temp. (°F)	Temp. at the point between two SWB's (°F)	Total SWB heat source (watts/SWB)	Radiolytic heat (watts/SWB)	Reaction heat* (watts/drum)
2Q-2014	74.0	138.1	40.5	1.16	19.67
3Q-2015	81.5	111.1	11.7	1.16	5.27
4Q-2016	56.5	88.1	6.8	1.16	2.82
2Q-2017	72.0	106.5	13.5	1.16	6.17

Note: [++]The upper SWB does not contain any reaction heat.
* The lower SWB contains two WCS 55-gallon drums with reaction heat source.
** Solar heat source [5]

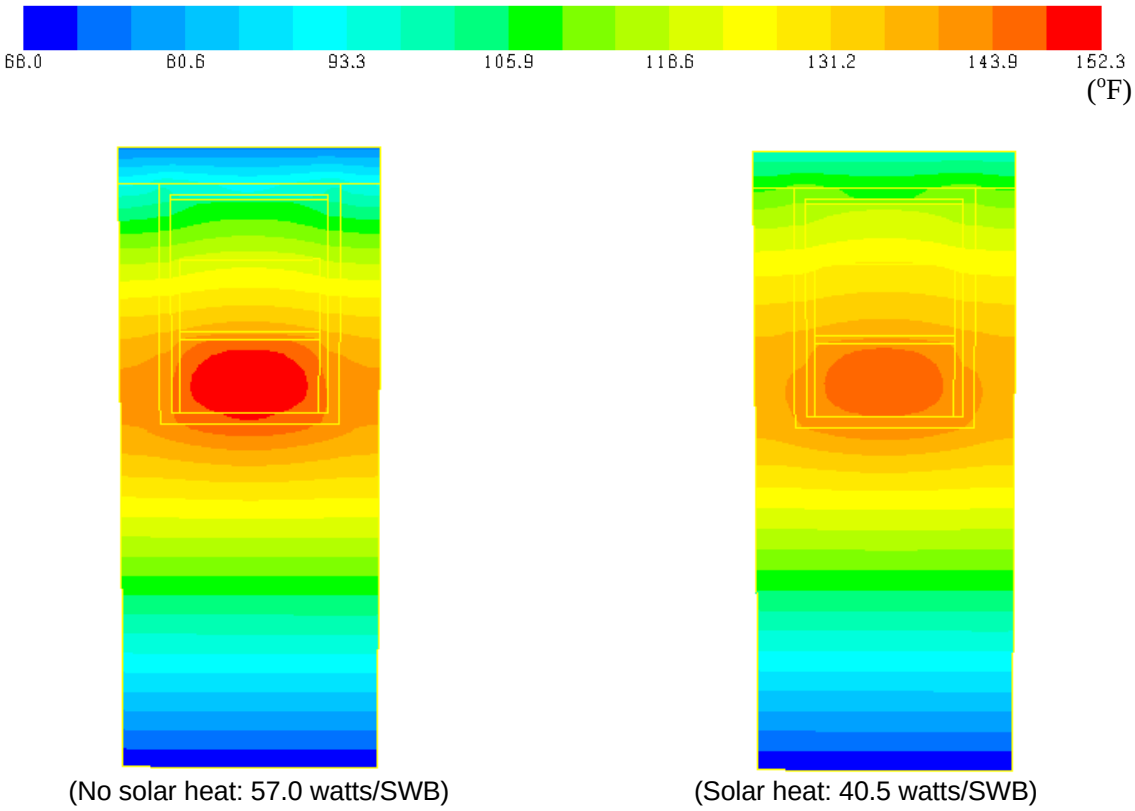

Figure 9. Comparison of the steady-state temperature distributions for the vertical mid plane between the cases with and without solar heat on the ground surface when temperature probe indicates 138 ºF in an ambient temperature 74 ºF (2Q-2014).

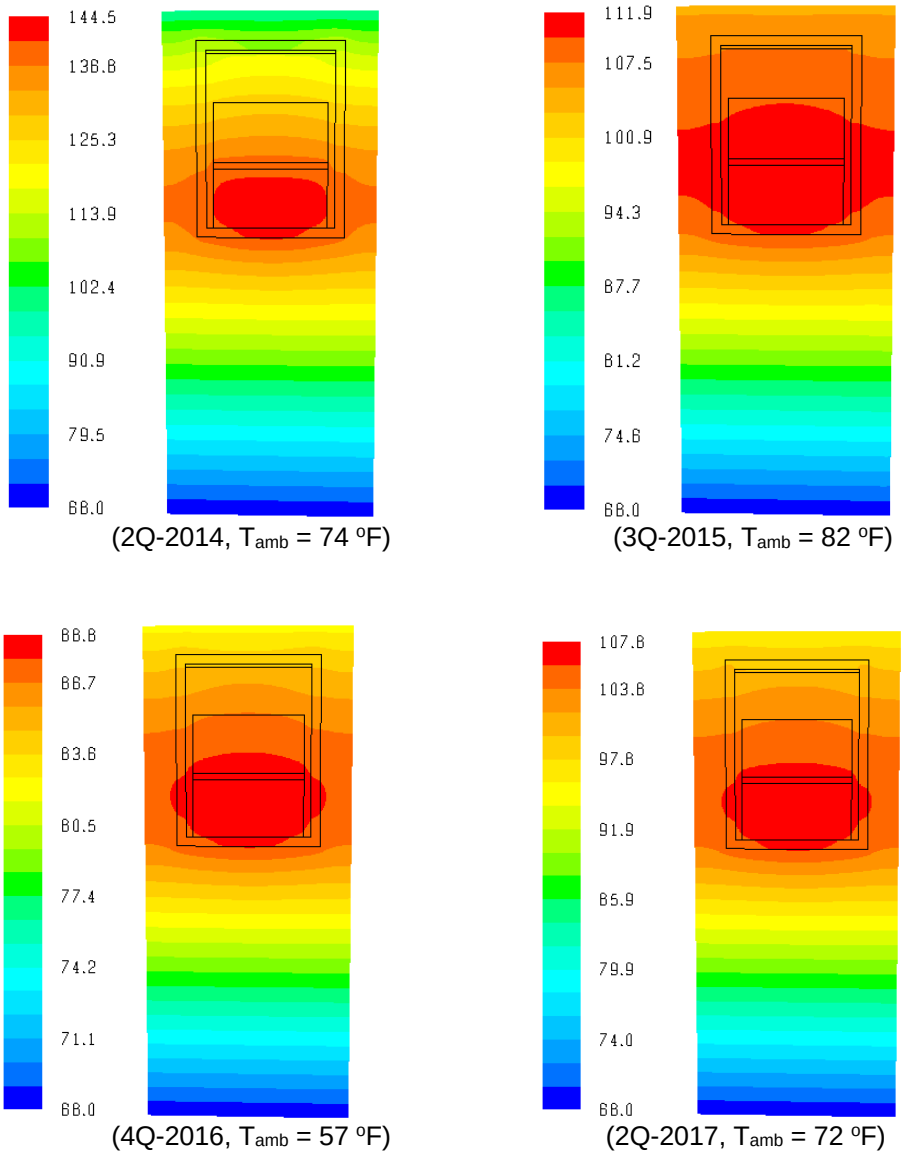

Figure 10. Comparison of the steady-state temperature distributions for the vertical mid-plane among the four cases with solar heat at the ground surface. (All the color codes are denoted in ºF.)

Table 7. Results of modeling calculations for the 2Q-2014 test case based on the symmetrical model as shown in Fig. 4

Cases	Measured values (Mean temperature)		Modeling predictions	
			No solar heat	Solar heat*
	Ambient air temperature (°F)	Temp at the point between two SWBs (°F)	Lower SWB heat source (watts/SWB)	Lower SWB heat source (watts/SWB)
2Q-2014	74.0	138.1	57.0	40.5

Note:* Solar heat source [5]

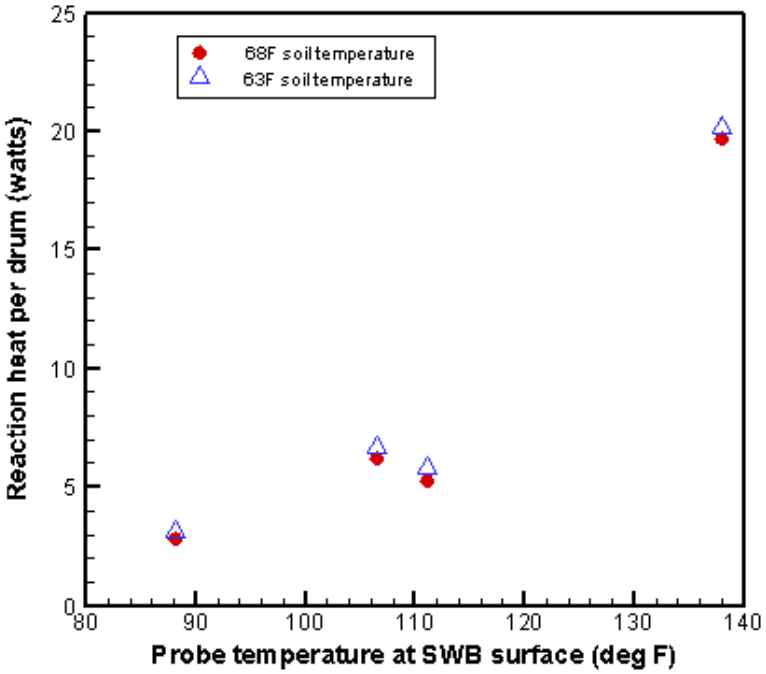

Figure 11. Comparison of the reaction drum heats for two different soil boundary temperatures

Table 8. Sensitivity results with repect to the nominal soil boundary condition of 68 °F as provided in Table 4

Cases	Measured values (Mean temperature)		Modeling predictions for the lower SWB heat source*	
	Ambient air temperature (°F)	Temp at the point between two SWBs (°F)	Nominal case: 68°F soil boundary (watts/SWB)	Sensitivity case: 63°F soil boundary (watts/SWB)
2Q-2014	74.0	138.1	40.5	41.5
3Q-2015	81.5	111.1	11.7	12.8
4Q-2016	56.5	88.1	6.8	7.8
2Q-2017	72.0	106.5	13.5	14.5

Note:* Solar heat source [5]

Table 9. Sensitivity results for reaction heats with respect to the assumed thermal conductivity of waste contents (0.65 watts/m-K) under solar condition*

Cases	Measured values (Mean temperature)		Modeling predictions for the lower SWB heat source**	
	Ambient air temperature (°F)	Temp. at the point between two SWBs (°F)	Assumed case of 0.65 watts/m-K (watts/SWB)	Sensitivity case of 0.45 watts/m-K (watts/SWB)
2Q-2014	74.0	138.1	40.5	39.5
3Q-2015	81.5	111.1	11.7	11.5
4Q-2016	56.5	88.1	6.8	6.6
2Q-2017	72.0	106.5	13.5	13.2

Note:* Solar heat source [5]
**The upper SWB does not contain any reaction heat source.

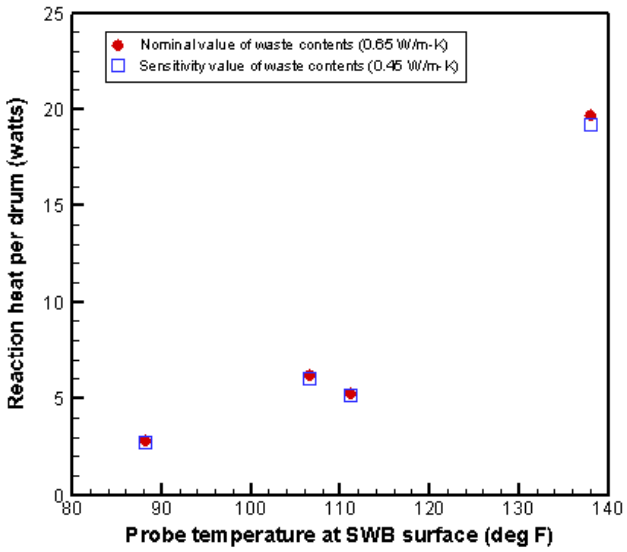

Figure 12. Comparison of the reaction drum heats for two different thermal conductivities of waste contents

Table 10. Sensitivity results for maximum temperatures with respect to the assumed thermal conductivity of waste contents (0.65 watts/m-K) under solar condition*

Cases	Measured values (Mean temperature)		Modeling predictions for maximum temperature	
	Ambient air temperature (°F)	Temp at the point between two SWBs (°F)	Assumed case of 0.65 watts/m-K (°F)	Sensitivity case of 0.45 watts/m-K (°F)
2Q-2014	74.0	138.1	144.5	146.3
3Q-2015	81.5	111.1	111.9	112.3
4Q-2016	56.5	88.1	88.8	89.0
2Q-2017	72.0	106.5	107.8	108.3

Note:* Solar heat source [5]

5.0 Conclusions

Three-dimensional steady-state CFD models were developed for thermal evaluations of the WCS drums when two SWBs are placed in an MCC. The primary objective of the work was to estimate the thermal heat source when WCS monitors the SWB package inside an interim storage facility of the MCC. Based on the basic modeling domain defined in Fig. 2 and the boundary conditions provided in Table 4, thermal calculations for four different test cases of SWBs in an MCC were made to estimate the heat source generated by the chemical reactions of the drum contents contained in the SWB when the SWB wall temperature measured by the thermocouple probe and ambient temperature of FWF are provided.

The computational model was benchmarked for a typical case representing the waste heat dissipation for a retrievable underground waste package because the test case is closely related to the underground cooling mechanism of WCS drums in an interim waste disposal facility of FWF. The results demonstrated that the modeling results are in excellent agreement with the theoretical results to within about 0.01%.

The symmetrical boundary conditions for the modeling domain were used for computational efficiency. In this case, an asymmetrical impact of the SWB geometry was assessed in terms of thermal performance by changing the asymmetrical geometry to the symmetrical one. For the symmetrical process, the SWB volume was kept unchanged for the same heat source. The assessment results show that thermal impact due to the symmetrical boundary of the prototypic SWB geometry was found to be negligible.

Based on the solution methodology and modeling conditions as benchmarked here, the performance results for the 2Q-2014 case showed that total heat source of 41 watts for waste contents of the lower SWB resulted in its wall temperature of 138 ^{o}F at ambient temperature of 74 ^{o}F during the insolated storage condition. When solar heat was not considered during the monitoring period, the steady state results for this case showed that the SWB package with heat source of 57 watts reached the measured temperature 138.1 ^{o}F at the probe point. It is noted that when the solar heat as provided in Table 4 was applied to the FWF ground surface, the measured temperature for the same case was reached at the SWB heat source about 16 watts lower than that of the shaded case. From

the thermal evaluations, it is noted that the reaction heat for the WCS drum contents ranges from about 3 watts to 20 watts when the SWB surface temperatures stored inside the interim MCC storage facility are in the range of 88 ^{o}F to 138 ^{o}F under solar condition.

When the thermal conductivity of the drum waste is changed from the assumed value of 0.65 W/m-K to the sensitivity value of 0.45 W/m-K, the raction heat of the WCS drum for the test cases done here results in no more than 0.5 watts smaller than the nominal value. The sensitivity results for the soil temperatures at the boundary indicated that when the soil temperature was 5^{o}F lower than the nominal value, total heat of the lower SWB was estimated to be about 1 watt higher than the nominal one for the insolated condition.

6.0 References

1. NRC Docket No. 70-7005, “WCS Safety Evaluation Report Regarding the Proposed Exemption from Requirements of 10 CFR Part 70”, November 2014.
2. S. M. Sayeed Bin Asad, Y. H. Shin, H. Chung, and H. Jeong, “Measurement of Ground Temperature Distribution at Various Depths”, Presented at the KSME2010 Conference, 2010.
3. Title 40 CFR Part 191 Subparts B and C, Compliance Recertification Application 2014 for the Waste Isolation Pilot Plant, Appendix DATA-2014, Attachment B: WIPP Waste Containers and Emplacement, United States Department of Energy, Carlsbad Field Office, Carlsbad, New Mexico.
4. H. Ozbek and S. L. Phillips, “Thermal Conductivity of Aqueous NaCl Solutions From 20^{o}C To 330^{o}C”, LBL-9086, Lawrence Berkeley Laboratory, University of California, Berkeley, 94720.
5. NASA’s Featured Article, “Earth’s Energy Budget”, Earth Observatory, NASA, *https://earthobservatory.nasa.gov/Features/EnergyBalance/page4.php*.
6. ANSYS-FLUENT User’s Guide, ANSYS, Inc., Canonsburg, Pennsylvania, 2012.
7. S. Y. Lee and R. A. Dimenna, “FLUENT Test & Verification Document”, WSRC-TR-2005-00563, Rev. 2, December 2009.
8. WIPP Container Data Reports:
   - WIPP Isolation Pilot Plant Container Data Report: Container Number LA00000055341, 6 February 2018.
   - WIPP Isolation Pilot Plant Container Data Report: Container Number LA00000069230, 6 February 2018.
   - WIPP Isolation Pilot Plant Container Data Report: Container Number LA00000068449, 6 February 2018.
   - WIPP Isolation Pilot Plant Container Data Report: Container Number LA00000069160, 6 February 2018.
   - WIPP Isolation Pilot Plant Container Data Report: Container Number LA00000063130, 6 February 2018.
   - WIPP Isolation Pilot Plant Container Data Report: Container Number LAS803015, 6 February 2018.
   - WIPP Isolation Pilot Plant Container Data Report: Container Number LA00000091281, 6 February 2018.

9. The Engineering ToolBox,"Emissivity Coefficients of Some Common Materials", *https://www.engineeringtoolbox.com/emissivity-coefficients-d_447.html*
10. The Engineering ToolBox, "Air – Thermophysical Properties", *https://www.engineeringtoolbox.com/air-properties-d_156.html*
11. The Engineering ToolBox, "Thermal Conductivity of Common Materials and Gases", *https://www.engineeringtoolbox.com/thermal-conductivity-d_429.html*
12. Jim Wilson, "Thermal Conductivity of Building Materials", Materials, Compounds, Adhesives, Substrates, No. 1, Technical Data, Vol. 14, February 1, 2008. *https://www.electronics-cooling.com/2008/02/thermal-properties-of-building-materials/*
13. G. Santa, F. Peron, A. Galgaro, M. Cultrera, D. Bertermann, J. Mueller, and A. Bernardi, "Laboratory Measurements of Gravel Thermal Conductivity: An Updated Methodological Approach", Energy Procedia, vol 125, pp. 671-677, 2017.
14. D. L. Wison, M. L. Baker, B. R. Hart, J. E. Marra, J. M. Schwantes, and P. E. Shoemaker, "Waste Isolation Pilot Plant Technical Assessment Team Report", SRNL-RP-2014-01198, Savannah River National Laboratory, March 17, 2017.
15. S. Y. Lee and D. W. Vinson, "Thermal Evaluations for L-Basin Drain-Down SNF Storage Facility", SRNL-STI-2016-00587, Savannah River National Laboratory, December 2016.

Distribution:

David.Dooley@srnl.doe.gov
Rudy.Goetzman@srnl.doe.gov
Bill.Wilmarth@srnl.doe.gov
Samuel.Fink@srnl.doe.gov
John.Young@srnl.doe.gov
Brian02.Looney@srnl.doe.gov
Aaron.Washington@srnl.doe.gov
Angela.Pizzino@srnl.doe.gov
Dave.Crowley@srnl.doe.gov
Luke.Reid@srnl.doe.gov
Matthew.Kesterson@srnl.doe.gov
Si.Lee@srnl.doe.gov